JACS
JOURNAL OF THE AMERICAN CHEMICAL SOCIETY
Communication
pubs.acs.org/JACS

Added Alkane Allows Thermal Thinning of Supramolecular Columns by Forming Superlattice—An X-ray and Neutron Study

Ming-Huei Yen,[†] Jitrin Chaiprapa,[†,#] Xiangbing Zeng,[†] Yongsong Liu,[‡] Liliana Cseh,[§,∥] Georg H. Mehl,[§] and Goran Ungar*[,‡,†]

[†]Department of Materials Science and Engineering, University of Sheffield, Sheffield S1 3JD, U.K.
[‡]Department of Physics, Zhejiang Sci-Tech University, Hangzhou 310018, China
[§]Department of Chemistry, University of Hull, Hull HU6 7RX, U.K.
[∥]Institute of Chemistry, Timisoara of Romanian Academy, Timisoara 300223, Romania

Supporting Information

ABSTRACT: We report a columnar superlattice formed by blends of dendron-like Li 3,4,5-tris(*n*-alkoxy)benzoates with *n*-alkanes. Without the alkane, the wedge-shaped molecules form liquid crystal columns with 3 dendrons in a supramolecular disk. The same structure exists in the blend, but on heating one dendron is expelled from the disks in every third column and is replaced by the alkane. This superlattice of unequal columns is confirmed by complementary X-ray and neutron diffraction studies. Lateral thermal expansion of dendrons normally leads to the expulsion of excess molecules from the column, reducing the column diameter. However, in the already narrow columns of pure Li salt, expulsion of one of only three dendrons in a disk is not viable. The added alkane facilitates the expulsion, as it replaces the missing dendron. Replacing the alkane with a functional compound can potentially lead to active nanoarrays with relatively large periodicity by using only small molecules.

Taper-shaped mesogens, notably dendrons, are some of the most fundamental and widespread building blocks in supramolecular chemistry.[1] They have been attached to moieties such as organic semiconductors,[2] fullerenes,[3] ionic conductors,[4] etc. This way "dendronized" functional materials may be created that can be used in a variety of applications.[5,6] The most common supramolecular objects that such dendrons or dendronized compounds form are columns and spheres. The former, in turn, tend to arrange on a 2-d lattice, most often hexagonal (Figure 1a), while the latter form 3-d lattices or even quasicrystals.[7,8] The most widely used dendrons producing 2-d and 3-d ordered liquid crystal (LC) or soft crystal structures consist of an aromatic core and flexible terminal chains. While dendrons of this type up to fifth generation have been synthesized and studied,[1] it turned out that most LC phases are observed already with the simplest tapered mesogens, the so-called "minidendrons", containing just one benzene ring, a weekly interacting group at the apex (1-position) and three or two flexible chains attached to positions 3, 4 and/or 5. The group at the apex could be carboxylate salt[9,10] sulfonate salt,[11] an onium group[4b,e] or other.

It is known that in the hexagonal columnar (Col_h) phase the columns consisting of tapered mesogens shrink in diameter on heating.[9,12] This has been explained by the taper angle φ increasing with increasing temperature (T) due to lateral expansion of the flexible alkyl chains caused by their increased conformational disorder. For any specific dendron at a given T there is an optimal number of molecules $\mu \approx 2\pi/\varphi$ required to complete the full disk. As a result of increasing φ with increasing T, the number of dendrons μ decreases and the excess dendrons are ejected from the columns; these then aggregate to form new columns. As a consequence on heating the average diameter of all columns decreases steadily.[9] Similar behavior is also observed in the cubic LC phase, where the number μ of conical dendrons in a spherical micelle decreases with increasing temperature, causing 3-d shrinkage of the unit cell.[9] Nevertheless, the bulk thermal expansivity of both the columnar and the cubic phases remains positive.

Here we report on rather unusual behavior of the columnar phase of some taper-shaped "minidendron" alkali metal salts of 3,4,5-tris(dodecyloxy)benzoic acid. While the columns of most salts become thinner when heated, those of Li salt change little, in fact expand slightly. Surprisingly, however, when free *n*-alkane is added, above a certain temperature the column diameter starts to decrease abruptly concomitant with the transition to a new superlattice phase. Using deuterated alkane and a combination of X-ray and neutron diffraction, we arrive at a detailed structure and a rationale for the formation of this unusual superlattice. The findings illuminate the intriguing phenomenon of "thinning" and "non-thinning" columns.

The "minidendrons" used in this work, referred to hereafter as "dendrons" for short, are shown in Scheme 1. The synthesis of the symmetrical dendrons was described previously,[9,10] while that of **12−12−18Li** is new. The details are given in Supporting Information (SI). All three compounds show a crystalline phase at low temperatures, followed by the Col_h phase on heating, then by the BCC cubic phase (see SI). Changes in the hexagonal lattice parameter a_h with temperature for 12−12−12Rb and 16−16−16Rb are shown in Figure 1b. They are given as examples of the steep decrease in column diameter, or intercolumnar distance (= a_h) on heating, typical for Na, K, Rb

Received: February 1, 2016
Published: April 22, 2016

DOI: 10.1021/jacs.6b01172
J. Am. Chem. Soc. 2016, 138, 5757−5760

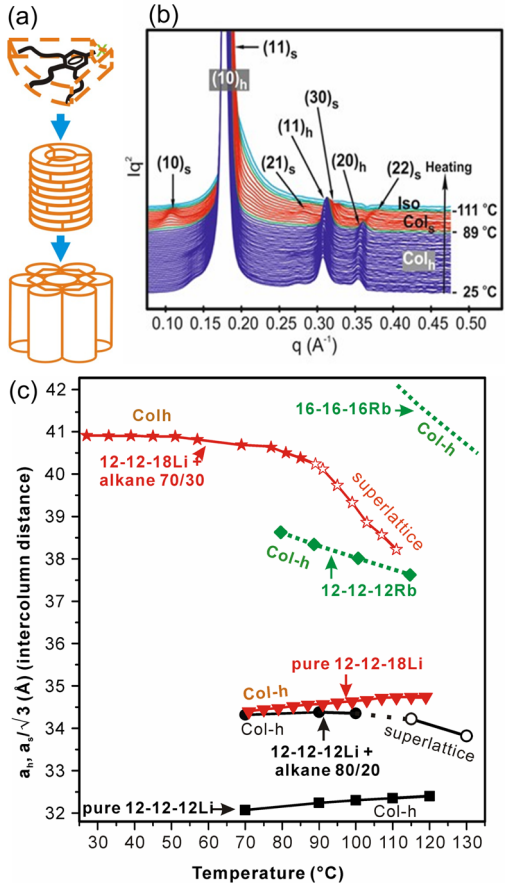

Figure 1. (a) Self-assembly of dendrons in a columnar phase (schematic). (b) SAXS curves for 12−12−18Li + $C_{19}D_{40}$ 70/30 recorded during first heating. SAXS experiments were done at beamline I22 at Diamond, UK. (c) Temperature dependence of intercolumnar distance in Col_h and Col_s phases of 12−12−12Rb, 12−12−12Li, 12−12−18Li, 12−12−12Li + $C_{19}D_{40}$ 80/20 and 12−12−18Li + $C_{19}D_{40}$ 70/30. The trendline for 16−16−16Rb from ref 9 is also added.

Scheme 1. Chemical Structure of the 3,4,5-Tris(*n*-Alkoxy)benzoate Salts Used[a]

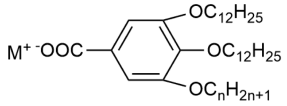

12-12-12Li: M = Li, n = 12	Cr 60 Col_h 130 BCC
12-12-18Li: M = Li, n = 18	Cr 70 Col_h 140 BCC
12-12-12Rb: M = Rb, n = 12	Cr 45 Col_h 120 LQC ...
12-12-12Li + $C_{19}D_{40}$ 80/20	Cr 25 Col_h 108 Col_s 135 Iso
12-12-18Li + $C_{19}D_{40}$ 70/30	Cr 25 Col_h 89 Col_s 111 Iso

[a]Transition temperatures (in °C) were determined by DSC and XRD on first heating. Cr = crystal, Col_h = hexagonal columnar, Col_s = columnar superlattice, BCC = body-centred cubic, LQC = dodecagonal quasicrystal. The ratios mean weight ratios in the blend.

and Cs salts.[9] In contrast, Li salts show no such decrease, and in fact the columns undergo slight lateral expansion. The plots of a_h vs T for pure 12−12−12Li and 12−12−18Li in the Col_h range are also shown in Figure 1c.

When an *n*-alkane is added to the dendron, a Col_h phase is observed again, but with an enlarged a_h. Within 5% error, the expansion of the unit cell can be fully accounted for by the added volume of the alkane. *n*-Alkanes $C_{15}H_{32}$, $C_{17}H_{36}$ and the perdeuterated $C_{19}D_{40}$ have all been found to show the same behavior. SAXS traces recorded at increasing T for 12−12−18Li + $C_{19}D_{40}$ 70/30 are shown in Figure 1b. The lattice parameter is plotted *vs* T in Figure 1c, both for this blend and for 12−12−12Li + $C_{19}D_{40}$ 80/20. At lower temperatures a remains nearly constant in both cases. However, at around 110 °C for 12−12−12Li + $C_{19}D_{40}$ 80/20 and at around 90 °C for 12−12−18Li + $C_{19}D_{40}$ 70/30 a starts to decrease relatively steeply and quite suddenly. This is particularly clear for 12−12−18Li + $C_{19}D_{40}$ 70/30, both from Figures 1b and 1c. We note that when the net bulk thermal expansion is taken into account, and considering that all expansion is confined to the *xy* plane (see below and Figure S7), a significant increase in a would be expected on heating; e.g., in 12−12−12Li + $C_{19}D_{40}$ 80/20 the expected increase between 70 and 130 °C would be 2.5%. On the basis of this, a should increase from 34.3 to 35.0 Å (see Table S4); instead it decreases to 33.8 Å (Figure 1b), a drop by 3.6% linear, or 7% in area and volume, from the expected value.

The other significant observation is that, at the point where the lattice starts to contract, additional relatively weak X-ray diffraction peaks appear, denoted $(10)_s$ and $(21)_s$ in Figure 1b. These additional reflections, together with the ones carried over from the low-T Col_h phase, can all be indexed on a 2-d hexagonal superlattice with a unit cell parameter $a_s = \sqrt{3}a_h$, (see Table S1), where a_h and a_s refer, respectively, to the low-T Col_h, and the high-T superlattice Col_s. As the extra reflections of the superlattice are weak, and the area of the Col_s unit cell is 3 times that of the Col_h cell, it is likely that the superlattice cell contains three columns that are similar but not identical. To test this conjecture we reconstructed electron density (ED) maps of the Col_h and Col_s phases using the intensities of the Bragg peaks, e.g., in Figure 2a,b—for details see SI.

The preferred maps for 12−12−12Li + $C_{19}D_{40}$ 80/20 are shown in Figures 2c and e, respectively, for the Col_h phase at 70 °C and Col_s phase at 130 °C. The high density in the center of the columns (purple) comes from the electron-rich aromatic cores, while the electron-poor aliphatic chains form the surrounding low-density continuum (red). As can be seen, in the superlattice (Figure 2e) two out of three columns in the cell have a high density core, while the density of the third is apparently lower. However, due to the ambiguity of the phase choice in the construction of ED maps, solely on the basis of XRD we could not exclude the alternative model with one dendron-rich and two dendron-poor columns (see SI). However, the neutron diffraction data favor the former model in 12−12−12Li + $C_{19}D_{40}$ 80/20 quite conclusively (see below). At the same time, however, the latter model is the most likely scenario in the case of 12−12−18Li + $C_{19}D_{40}$ 70/30 at the highest temperature, as explained in SI.

The reason for using perdeuterated n-$C_{19}D_{40}$ is that neutrons can clearly distinguish it from the hydrogenous alkyl tails of the dendrons (Section 3 and Table S3). Experimental small-angle neutron and X-ray diffraction curves of 12−12−12Li + $C_{19}D_{40}$ 80/20 are compared in Figures 2a and 2b, respectively, for the Col_h and Col_s phase. As one can see, the X-ray and neutron diffractograms are very different: X-rays "see" the aromatic domains, while neutrons are most strongly scattered on the deuterated alkane and, to a lesser extent, on the aromatic regions (Table S3). Particularly striking is the relatively high intensity of the additional superlattice reflections in the neutron

DOI: 10.1021/jacs.6b01172
J. Am. Chem. Soc. 2016, 138, 5757−5760

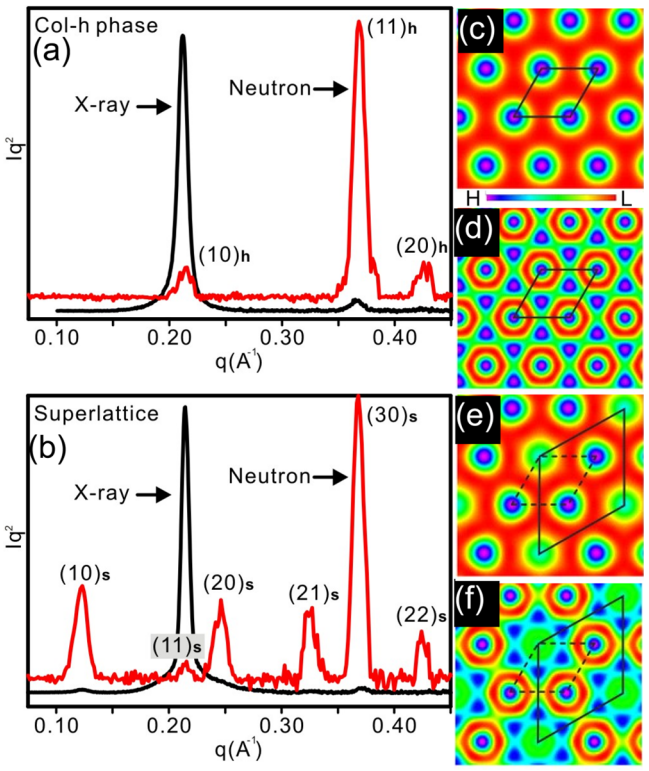

Figure 2. (a,b) Small-angle X-ray (black) and neutron powder diffractograms (red) of 12−12−12Li + $C_{19}D_{40}$ 80/20 in the (a) Col_h phase at 70 °C and (b) the superlattice phase at 130 °C. (c) ED and (d) neutron SLD map of the Col_h phase. (e) ED and (f) SLD map of the Col_s. Neutron experiments at station D16 at ILL, Grenoble.

pattern (labeled 10s, 20s, 21s, Figure 2b), suggesting a major rearrangement of the added alkane upon the Col_h-Col_s transition. The neutron scattering length density (SLD) maps are shown in Figures 2d and 2f for the Col_h and Col_s phases. For details of the construction of the maps see SI. Like the ED map, the SLD map of the Col_s phase also shows the presence of two different types of columns.

Next we proceed to determine the number of molecules in the unit cell and in each of the constituent columns. Both the Col_h and Col_s phases can be classed as "ordered" columnar phases and both have a molecular stacking periodicity c = 4.2 Å along the column axis, the same as that of pure 12−12−12Li. This is determined from the meridional reflection in the fiber patterns (Figures S7 and S8). From the calculated unit cell volume and material density the number of molecules in the cell has been derived for pure 12−12−12Li and the 12−12−12Li + $C_{19}D_{40}$ 80/20 mixture—see Tables S4 and S5. In pure 12−12−12Li there are μ = 3.2 molecules per unit cell (or column stratum). In the blend there are μ = 2.9 dendrons and ν = 1.6 alkane molecules in the average Col_h cell at 70 °C, and μ' = 7.9 dendrons and ν' = 4.4 alkanes in the superlattice cell at 130 °C. Rounded to the nearest integer, this gives $\mu \approx 3$ in the Col_h phases and $\mu' \approx 8$ in the superlattice.

Thus, a stratum, or molecular layer, in a column of the Col_h phase contains ca. three dendrons, the same as the pure 12−12−12Li salt. The SLD map of the Col_h phase in Figure 2d indicates that $C_{19}D_{40}$ (high SLD) preferentially settles in the interstices between each three neighboring columns. This accounts for the six purple SLD maxima surrounding each column in Figure 2d, the maximum in the column center being mainly due to the aromatic rings (see Table S3).

In order to determine the number of dendrons in the two column types in the superlattice, we integrate the excess electron density of the column cores above the ED of the aliphatic background in the map in Figure 2e. Thus, we obtain for the Col_s of 12−12−12Li + $C_{19}H_{40}$ 80/20 at 130 °C, 1.57 as the ratio between the number of molecules in the dendron-rich (purple) and dendron-poor (green) columns. Thus, there are ca. 3 dendrons in each of the two dendron-rich columns and 2 dendrons in the remaining dendron-deficient column in the unit cell, totaling 3 + 3 + 2 = 8 dendrons.

The situation in one stratum of the two phases is depicted schematically in Figures 3a and b. In view of the above model,

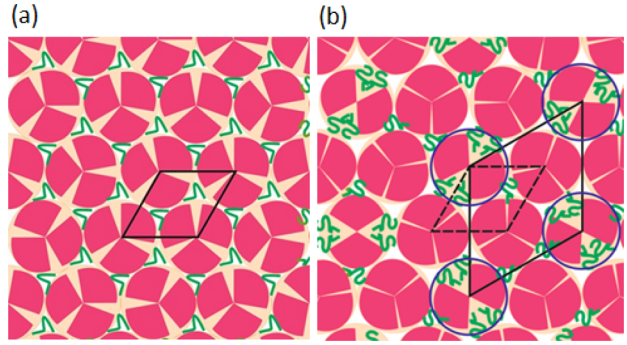

Figure 3. Schematic model of a layer of the 12−12−12Li + $C_{19}D_{40}$ 80/20 blend in the (a) Col_h and (b) superlattice phase (pink: minidendrons; green: *n*-alkane).

the neutron SLD map in Figure 2f is easily understood. As in the Col_h phase, there are still six SLD maxima surrounding each column due to $C_{19}D_{40}$ clustering in the triangular channels. But notably the dendron-deficient columns have now lost their central SLD maximum as well as the low-density circle around it. The former is explained by the lowering of the total scattering cross-section of the column center due to the missing dendron with its aromatic ring. The latter, i.e., the filling of the low-density ring, is explained by the high-SLD deuterated alkane replacing the low-SLD hydrogenous alkyl tails of the missing dendron.

As shown in SI, the neutron SLD map of 12−12−12Li + $C_{19}D_{40}$ 80/20 at 130 °C proves conclusively that the arrangement in the Col_s unit cell is "2·3 + 1·2", i.e., two 3-dendron columns and one 2-dendron column. However, such configuration cannot be ascertained for the Col_s phase at all compositions of the blend. For a smaller alkane percentage the dendron-deficient column may contain a mixture of two-dendron and three-dendron strata. More significantly, in the case of the 12−12−18Li + $C_{19}D_{40}$ 70/30 blend at the highest temperature of 112 °C (see Figure 1c) the calculated number of dendrons in a Col_s cell is only 7; there a "2·3 + 1·2" arrangement is impossible, and it is likely that instead a "1·3 + 2·2" configuration is adopted. Thus, dendron-deficient columns that are strictly uniform, i.e., with all strata having the same integer number of dendrons, cannot be maintained at all temperatures.

As already discussed, adding alkane to the Li salts makes it possible for a unit stratum to eject a dendron by partially replacing it with the alkane. However, questions, such as why a superlattice is formed and why 3-dendron and 2-dendron cells are not distributed randomly, are still to be addressed. We

DOI: 10.1021/jacs.6b01172
J. Am. Chem. Soc. 2016, 138, 5757−5760

propose that by grouping all smaller 2-dendron strata in a separate column the overall lattice strain can be minimized. Thus, we might think of the superlattice as a network of line dislocations, with the deficient strata all grouped in an array of lines.

The remaining question to answer is why the columns of the Li salts do not show thermal contraction like the other alkali metal salts,[9] exemplified here by 12−12−12Rb and 16−16−16Rb (Figure 1c). We propose that the columns of the Li salts resist contraction because with the number (μ) of dendrons as small as three, the loss of one dendron would create unoccupied space that the expanding tails of the remaining two dendrons could not fill at any temperature within the range of the Col_h phase. Thus, without added alkane, lateral contraction could not occur for Li salts. By contrast, in the salts of other alkali metals μ is larger than 3 (in 12−12−12Rb and 16−16−16Rb μ is close to 4), hence the loss of one molecule leaves a proportionally smaller gap that the remaining dendrons could fill. Moreover, the Col_h phase in the salts with larger cations is of the "disordered" type, i.e., a true liquid crystal and not a "soft crystal" with a degree of 3-d order. As can be seen in the fiber pattern of 12−12−12Rb in Figure S8, there is no sharp Bragg diffraction on or near the meridian, hence no periodic π-stacking. Such disordered columnar structures are more likely to tolerate a noninteger μ. We also add that the column thinning is partially reversible (see Figure S9).

In conclusion, we have presented a new type of superlattice in liquid crystals. At the thermal transition from the simple hexagonal to the superlattice columnar phase the added alkane diluent is redistributed into an ordered array of dendron-deficient columns. This mitigates the large relative drop from 3 to 2 in the number of dendrons per stratum. The results shed new light on the intriguing phenomena of heat-thinning columns and supramolecular superlattices. This new type of superlattice also shows the way to distribute a potentially active functional additive in an ordered 2-D pattern of sizable period using only small molecules.

■ ASSOCIATED CONTENT

Supporting Information

The Supporting Information is available free of charge on the ACS Publications website at DOI: 10.1021/jacs.6b01172.

DSC; X-ray and neutron experimental and additional data; density maps; calculation; molecular modeling. (PDF)

■ AUTHOR INFORMATION

Corresponding Author

*g.ungar@sheffield.ac.uk

Present Address

#Synchrotron Research Inst., Nakhon Ratchasima, Thailand.

Notes

The authors declare no competing financial interest.

■ ACKNOWLEDGMENTS

For help with synchrotron SAXS and neutron experiments we thank Prof. N. Terrill at I22, Diamond, and Drs. A. Perkins and B. Deme at D16, ILL. Financial support is acknowledged from NSF-EPSRC project "RENEW" (EP/K034308), EPSRC (EP/D058066), Leverhulme Trust (RPG-2012-804), NSFC China (21274132).

■ REFERENCES

(1) (a) Sun, H.-J.; Zhang, S.; Percec, V. *Chem. Soc. Rev.* **2015**, *44*, 3900. (b) Donnio, B.; Buathong, S.; Bury, I.; Guillon, D. *Chem. Soc. Rev.* **2007**, *36*, 1495−1513. (c) Tschierske, C. *Angew. Chem., Int. Ed.* **2013**, *52*, 8828−8878. (d) Kato, T.; Mizoshita, N.; Kishimoto, K. *Angew. Chem., Int. Ed.* **2006**, *45*, 38−68.

(2) (a) Würthner, F.; Thalacker, C.; Diele, S.; Tschierske, C. *Chem. - Eur. J.* **2001**, *7*, 2245−2253. (b) An, Z.; Yu, J.; Domercq, B.; Jones, S. C.; Barlow, S.; Kippelen, B.; Marder, S. R. *J. Mater. Chem.* **2009**, *19*, 6688−6698. (c) Percec, V.; Peterca, M.; Tadjiev, T.; Zeng, X.; Ungar, G.; Leowanawat, P.; Aqad, E.; Imam, M. R.; Rosen, B. M.; Akbey, U.; Graf, R.; Sekharan, S.; Sebastiani, D.; Spiess, H. W.; Heiney, P. A.; Hudson, S. D. *J. Am. Chem. Soc.* **2011**, *133*, 12197−12219.

(3) (a) Li, W. S.; Yamamoto, Y.; Fukushima, T.; Saeki, A.; Seki, S.; Tagawa, S.; Masunaga, H.; Sasaki, S.; Takata, M.; Aida, T. *J. Am. Chem. Soc.* **2008**, *130*, 8886. (b) Nierengarten, J.-F.; Oswald, L.; Eckert, J.-F.; Nicoud, J.-F.; Armaroli, N. *Tetrahedron Lett.* **1999**, *40*, 5681.

(4) (a) Ungar, G.; Batty, S. V.; Percec, V.; Heck, J.; Johansson, G. *Adv. Mater. Opt. Electron.* **1994**, *4*, 303−313. (b) Ichikawa, T.; Yoshio, M.; Hamasaki, A.; Mukai, T.; Ohno, H.; Kato, T. *J. Am. Chem. Soc.* **2007**, *129*, 10662−10663. (c) Peterca, M.; Percec, V.; Dulcey, A. E.; Nummelin, S.; Korey, S.; Ilies, M.; Heiney, P. A. *J. Am. Chem. Soc.* **2006**, *128*, 6713−6720. (d) Pecinovsky, C. S.; Hatakeyama, E. S.; Gin, D. L. *Adv. Mater.* **2008**, *20*, 174−178. (e) Soberats, B.; Yoshio, M.; Ichikawa, T.; Zeng, X. B.; Taguchi, S.; Ohno, H.; Liu, F.; Ungar, G.; Kato, T. *J. Am. Chem. Soc.* **2015**, *137*, 13212−13215.

(5) Feng, X.; Tousley, M. E.; Cowan, M. G.; Wiesenauer, B. R.; Nejati, S.; Choo, Y.; Noble, R. D.; Elimelech, M.; Gin, D. L. O.; Osuji, C. O. *ACS Nano* **2014**, *8*, 11977−11986.

(6) Feng, X.; Nejati, S.; Cowan, M. G.; Tousley, M. E.; Wiesenauer, B. R.; Noble, R. D.; Elimelech, M.; Gin, D. L. O.; Osuji, C. O. *ACS Nano* **2016**, *10*, 150−158.

(7) Ungar, G.; Zeng, X. B. *Soft Matter* **2005**, *1*, 95−106.

(8) Ungar, G.; Liu, F.; Zeng, X. B. In *Handbook of Liquid Crystals*, 2nd ed.; Goodby, J. W., Collins, P. J., Kato, T., Tschierske, C., Gleeson, H. F., Reynes, P., Eds.; VCH-Wiley: Weinheim, 2014; Vol. *5*, Chapter 7, pp 363−436.

(9) Ungar, G.; Percec, V.; Holerca, M. N.; Johansson, G.; Heck, J. A. *Chem. - Eur. J.* **2000**, *6*, 1258−1266.

(10) Percec, V.; Holerca, M. N.; Uchida, S.; Cho, W. D.; Ungar, G.; Lee, Y. S.; Yeardley, D. J. P. *Chem. - Eur. J.* **2002**, *8*, 1106−1117.

(11) (a) Beginn, U.; Yan, L.; Chvalun, S. N.; Shcherbina, M. A.; Bakirov, A.; Möller, M. *Liq. Cryst.* **2008**, *35*, 1073−1093. (b) Shcherbina, M. A.; Bakirov, A.; Yakunin, A. N.; Beginn, U.; Yan, L.; Möller, M.; Chvalun, S. N. *Soft Matter* **2014**, *10*, 1746−1757.

(12) Kwon, J.-K.; Chvalun, S. N.; Blackwell, J.; Percec, V.; Heck, J. A. *Macromolecules* **1995**, *28*, 1552−1558.

DOI: 10.1021/jacs.6b01172
J. Am. Chem. Soc. 2016, 138, 5757−5760